



Article

Protective Effect of *Colla corii asini* against Lung Injuries Induced by Intratracheal Instillation of Artificial Fine Particles in Rats

Tiantian Liu ^{1,2} , Piaopiao Zhang ², Yahao Ling ², Guang Hu ², Jianjun Gu ³, Hong Yang ⁴, Jinfeng Wei ^{2,5}, Aiping Wang ^{2,5} and Hongtao Jin ^{2,5,*}

- ¹ State Key Laboratory of Bioactive Substance and Function of Natural Medicines, Institute of Materia Medica, Chinese Academy of Medical Sciences & Peking Union Medical College, Beijing 100050, China; liutiantian@imm.ac.cn
- ² New Drug Safety Evaluation Center, Institute of Materia Medica, Chinese Academy of Medical Sciences & Peking Union Medical College, Beijing 100050, China; purepiao123@gmail.com (P.Z.); lingyahao1990@163.com (Y.L.); huguang@imm.ac.cn (G.H.); weijinfeng@imm.ac.cn (J.W.); wangaiping@imm.ac.cn (A.W.)
- ³ National Engineering Research Center for Gelatin-based Traditional Chinese Medicine, Shandong 252299, China; gujj@dongeejiao.com
- ⁴ Experimental Research Center, China Academy of Chinese Medical Sciences, Beijing 100700, China; yanghong@merc.ac.cn
- ⁵ Beijing Union-Genius Pharmaceutical Technology Co., Ltd., Beijing 100176, China
- * Correspondence: jinhongtao@imm.ac.cn; Tel.: +86-10-67817730; Fax: +86-10-67817731

Received: 13 November 2018; Accepted: 20 December 2018; Published: 23 December 2018



Abstract: Environmental issues pose huge threats to public health, particularly the damage caused by fine particulate matter (PM_{2.5}). However, the mechanisms of injury require further investigation and medical materials that can protect the lungs from PM_{2.5} are needed. We have found that *Colla corii asini*, a traditional Chinese medicine that has long been used to treat various ailments, is a good candidate to serve this purpose. To understand the mechanisms of PM_{2.5}-induced lung toxicity and the protective effects of *Colla corii asini*, we established a rat model of lung injury via intratracheal instillation of artificial PM_{2.5} (aPM_{2.5}). Our results demonstrated that *Colla corii asini* significantly protected against lung function decline and pathologic changes. Inflammation was ameliorated by suppression of *Arg-1* to adjust the disturbed metabolic pathways induced by aPM_{2.5}, such as arginine and nitrogen metabolism and aminoacyl-tRNA biosynthesis, for 11 weeks. Our work found that metabolomics was a useful tool that contributed to further understanding of PM_{2.5}-induced respiratory system damage and provided useful information for further pharmacological research on *Colla corii asini*, which may be valuable for therapeutic intervention.

Keywords: *Colla corii asini*; artificial fine particles; intratracheal instillation; lung injury; metabolomics

1. Introduction

Air pollution, particularly fine particles (particles with a mass median aerodynamic diameter of less than 2.5 μm , PM_{2.5}), has become a major environmental issue affecting public health globally [1–3]. Although air quality-control policies have been implemented by the Chinese government, the levels of PM_{2.5} in China remain substantially higher than those in developed countries and have become a significant threat to people living on the mainland [4–6]. Studies suggest that short- and long-term exposure to PM_{2.5} are linked to a range of negative health outcomes, including respiratory disorders [7], cardiovascular and cerebrovascular diseases [8] and decreased life expectancy [9,10].

Colla corii asini (E'jiao, donkey-hide gelatin), a traditional Chinese medicinal preparation that has been used for more than 2000 years, is the solid glue prepared from the skin of *Equus asinus* by boiling and concentration. The main components are amino acids and microelements, as well as small molecular weight hydrolysates of collagen proteins that are included in the medical material. It has been reported to possess a variety of clinical functions in terms of hematopoiesis, enhancement of cellular immunity and radio-protection [11–14]. Recent reports have shown that *Colla corii asini* has anti-inflammation properties and can stimulate both specific and non-specific immune function in hypimmune mice. Zhang showed that *Colla corii asini* reversed the imbalance of Th17/Treg subsets in mice with airway inflammation [15,16]. Our previous study showed that *Colla corii asini* prevented oxidative damage caused by aPM_{2.5} [17]. These results collectively suggest that *Colla corii asini* may be a useful therapeutic agent to protect against pulmonary impairment.

The mechanisms underlying PM_{2.5}-induced lung toxicity/pulmonary impairment still need further study. To explore this issue, artificial PM_{2.5} particles (aPM_{2.5}) were created based on the physical and chemical properties of PM_{2.5} particles collected in Beijing [18]. We investigated the protective effects and mechanism of action of *Colla corii asini* in an 11-week study of respiratory system injury induced by intratracheal instillation of aPM_{2.5} in rats.

2. Results

2.1. *Colla corii asini* Protects Rats from aPM_{2.5}-Induced Lung Function Changes

The rats were exposed to aPM_{2.5} (30 mg/kg, 1 mL/kg body weight) via intratracheal instillation except for the controls, while rats in the aPM_{2.5} + *Colla corii asini* groups received *Colla corii asini* daily by oral gavage for 11 weeks at doses of 1, 2 and 5 g/kg body weight. Respiratory function of all animals was measured weekly throughout the treatment for 11 weeks. As shown in Figure 1A–D, compared with those in the control group, the tidal volume, expiratory volume, minute ventilation volume and expiratory flow at 50% tidal volume of the aPM_{2.5} group were significantly increased between 8 and 11 weeks. Treatment with *Colla corii asini* significantly suppressed these volume parameters (* $p < 0.05$ or ** $p < 0.01$). The inspiratory time, end-inspiratory time and respiratory rate of aPM_{2.5}-treated rats decreased (Figure 1E,F,I) with respect to the control group but these parameters were increased in the aPM_{2.5} + *Colla corii asini* groups (* $p < 0.05$ or ** $p < 0.01$). Airway resistance was increased after intratracheal instillation of aPM_{2.5} between 4 and 11 weeks, as evidenced by the change in flow index of the ventilation function, including increases in peak inspiratory and expiratory flow. After *Colla corii asini* treatment, these indices significantly rebounded (* $p < 0.05$ or ** $p < 0.01$), with values similar to those of controls (Figure 1G,H). Intratracheal instillation of aPM_{2.5} induced a time-dependent reduction of lung function. Treatment of aPM_{2.5}-exposed rats with *Colla corii asini* (1, 2, or 5 g/kg, oral) for 11 weeks provided a significant protective effect against aPM_{2.5}-induced lung function changes.

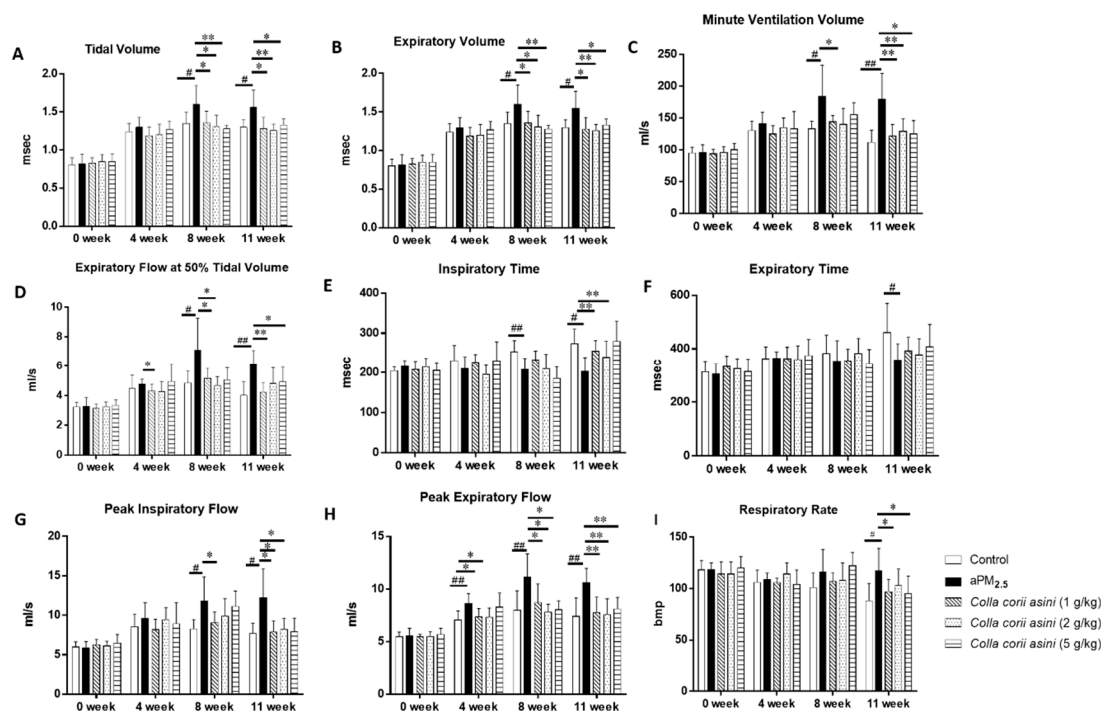


Figure 1. Protective effect of *Colla corii asini* in rats subjected to intratracheal instillation of aPM_{2.5}. (A–I) Respiratory function changes of rats during intratracheal instillation of aPM_{2.5} for 11 weeks. (A). Tidal volume and (B). Expiratory volume (msec). (C). Minute ventilation volume. (D). Expiratory flow at 50% tidal volume (mL). (E). Inspiratory time and (F). Expiratory time (msec). (G). Peak inspiratory flow. (H). Peak expiratory flow (mL/s). (I). Respiratory rate (bmp). # $p < 0.05$ and ## $p < 0.01$, versus the control group; * $p < 0.05$ and ** $p < 0.01$, versus the aPM_{2.5} group, $n = 8$.

2.2. Effect of *Colla corii asini* on aPM_{2.5}-Induced Alteration of T Lymphocyte Subsets

The T lymphocyte profiles (Table 1) were not significantly different between the control and aPM_{2.5} groups in the fresh whole blood of rats of 11 weeks. However, *Colla corii asini* decreased CD8⁺ level in the presence of aPM_{2.5}. Compared with the aPM_{2.5} group, the CD4⁺/CD8⁺ ratio increased in the *Colla corii asini* + aPM_{2.5} groups.

Table 1. Role of *Colla corii asini* in aPM_{2.5}-induced alteration of T lymphocyte subsets.

Group	<i>Colla corii asini</i> (g/kg)	Number	CD3 ⁺ (%)	CD4 ⁺ (%)	CD8 ⁺ (%)	CD4 ⁺ /CD8 ⁺
Control	-	8	55.29 ± 9.46	44.63 ± 8.89	10.26 ± 3.31	4.84 ± 2.06
aPM _{2.5}	-	8	54.69 ± 5.52	44.44 ± 5.50	10.16 ± 4.56	5.54 ± 3.09
Low-dose group	1	8	51.28 ± 5.26	44.36 ± 5.49	6.18 ± 2.55 ^{#,*}	8.48 ± 3.70 [#]
Mid-dose group	2	8	58.44 ± 8.44	48.14 ± 10.1	7.01 ± 4.83	8.22 ± 3.47 [#]
High-dose group	5	8	54.18 ± 4.79	47.07 ± 5.08	6.79 ± 2.93	8.95 ± 5.98 [#]

Data are presented as the mean ± SD. # $p < 0.05$, significant difference between *Colla corii asini*-treated groups and control group; * $p < 0.05$, significant difference between *Colla corii asini*-treated groups and aPM_{2.5}-treated group.

2.3. Effect of *Colla corii asini* on Cell Counts and Percentages

Indicative of lung inflammation, significant increases in total white blood cell (WBC), lymphocyte (LYM), monocyte (MON), neutrophil (NEUT) and eosinophil (EOS) counts in BALF week 11 samples were observed in the aPM_{2.5}-exposed rats compared with the controls (Figure 2A, ## $p < 0.01$). The most pronounced increases were in the LYM% and BAS% counts (Figure 2B, # $p < 0.05$). *Colla corii asini* treatment reversed these changes compared to the aPM_{2.5} group (* $p < 0.05$ or ** $p < 0.01$).

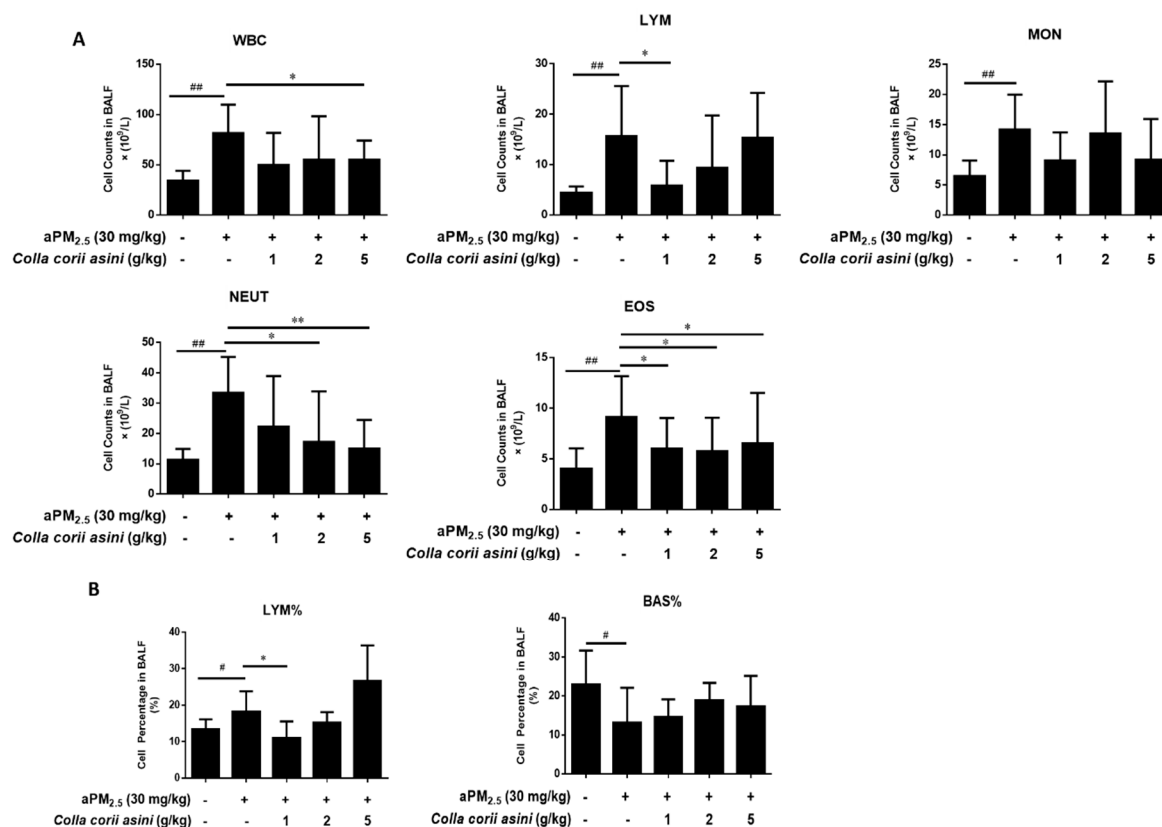


Figure 2. *Colla corii asini* prevented aPM_{2.5}-induced inflammation. Effects of *Colla corii asini* on (A), cell counts (× 10⁹/L) and (B), cell percentage in the BALF of rats subjected to intratracheal instillation of aPM_{2.5} for 11 weeks. Data are expressed as mean ± SD (n = 8). # p < 0.05 and ### p < 0.01, versus the control group; * p < 0.05 and ** p < 0.01, versus the aPM_{2.5} group.

2.4. Effect of *Colla corii asini* on Protein and mRNA Expression of TNF- α , IL-1 β and IL-10

As shown in Figure 3A, aPM_{2.5} caused increased production of pro-inflammatory cytokines, including TNF- α and IL-1 β (### p < 0.01) and a decrease of anti-inflammatory IL-10 (# p < 0.05) in BALF compared to the control rats. In particular, the high-dose of *Colla corii asini* decreased the protein level of TNF- α (* p < 0.05), while IL-1 β decreased as the *Colla corii asini* dose was increased (* p < 0.05 or ** p < 0.01) with respect to the aPM_{2.5} group. In addition, expression of these cytokine genes was also determined to further characterize the in vivo inflammatory response. Expression of TNF- α and IL-1 β mRNA were increased 2.27- (# p < 0.05) and 2.09-fold (# p < 0.05) in the lungs of the aPM_{2.5}-exposed rats at 11 weeks compared to the control group. The IL-10 mRNA expression was not affected by aPM_{2.5} (Figure 3B). Protein and mRNA expression of IL-10 were increased in *Colla corii asini*-treated groups but the changes were not statistically significant. These results suggest that *Colla corii asini* treatment suppressed pro-inflammatory cytokine production in the aPM_{2.5} model.

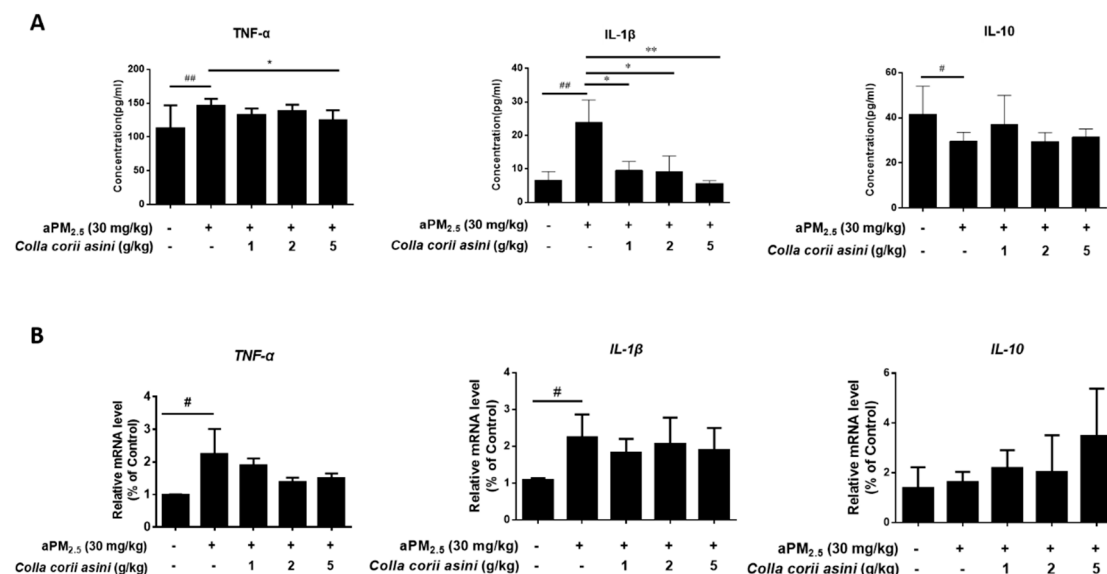


Figure 3. *Colla corii asini* prevented aPM_{2.5}-induced inflammation. Effect of *Colla corii asini* on (A). TNF- α , IL-1 β , IL-10 concentrations (pg/mL) in BALF (mean \pm SD, $n = 8$) and (B). relative gene expression of TNF- α , IL-1 β and IL-10 in the lungs of rats subjected to intratracheal instillation of aPM_{2.5} for 11 weeks. Values are reported using the $2^{-\Delta\Delta C_t}$ method and were obtained by comparison to those of the control group and normalized to β -actin (ACTB) (mean \pm SD, $n = 3$). # $p < 0.05$ and ### $p < 0.01$, versus the control group; * $p < 0.05$ and ** $p < 0.01$, versus the aPM_{2.5} group.

2.5. *Colla corii asini* Inhibits Pathologic Changes and Lung Injury in Rats

Compared with control group lungs, intratracheal instillation of aPM_{2.5} resulted in interstitial/alveolar wall thickening and emphysematous changes in lung sections from rats after aPM_{2.5} exposure in week 11, as shown in Figure 4. The rats receiving aPM_{2.5} developed inflammatory cell infiltration, characterized by neutrophil and lymphocyte infiltration, which was, however, suppressed by 5 g/kg body weight of *Colla corii asini*. The pathologic damage was milder in the aPM_{2.5} plus *Colla corii asini* groups than in the aPM_{2.5} group, with less thickness of local alveolar septae and decreased macrophages infiltration. The results indicated that *Colla corii asini* alleviated, to some extent, lung injury induced by intratracheal instillation of aPM_{2.5} for 11 weeks in rats.

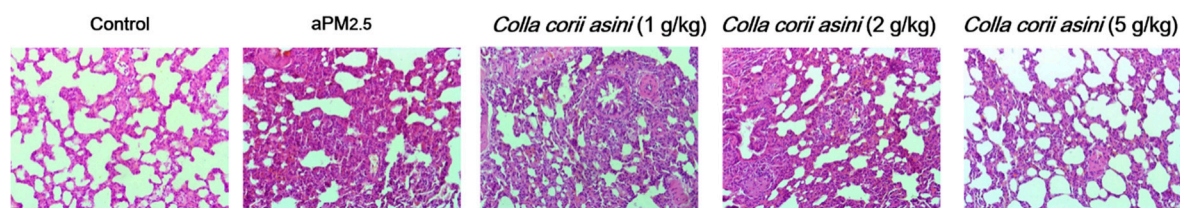


Figure 4. *Colla corii asini* prevented aPM_{2.5}-induced inflammation. H&E-stained ($\times 200$) lung sections from rats after aPM_{2.5} exposure for 11 weeks. Histological examination and representative images are shown.

2.6. Role of *Colla corii asini* in Protection against aPM_{2.5}-Induced Alteration of Amino Metabolic Profile

A number of potential biomarkers were identified and are listed in the supplementary material. From the score plots of the Principal Component Analysis (PCA) model (Figure S1) clear separation among the control, aPM_{2.5} and *Colla corii asini* groups was observed in lung tissue from rats subjected to intratracheal instillation of aPM_{2.5} in week 11. In this study, a total of six discriminating metabolites contributed to the classification of the control and aPM_{2.5} groups (Figure 5, Table S1). Comparison of the levels of identified biomarkers in the aPM_{2.5} and *Colla corii asini* groups revealed that four of them were reversed by *Colla corii asini*, as shown in Figure 6. An additional 24 metabolites were also

altered to different degrees (Table S1). All of the discriminating biomarkers belonged to the identified metabolic pathways. *Colla corii asini* displayed an obvious protective effect by adjusting the disturbed metabolic pathways, including arginine and proline metabolism, aminoacyl-tRNA biosynthesis and nitrogen metabolism by searching the KEGG database.

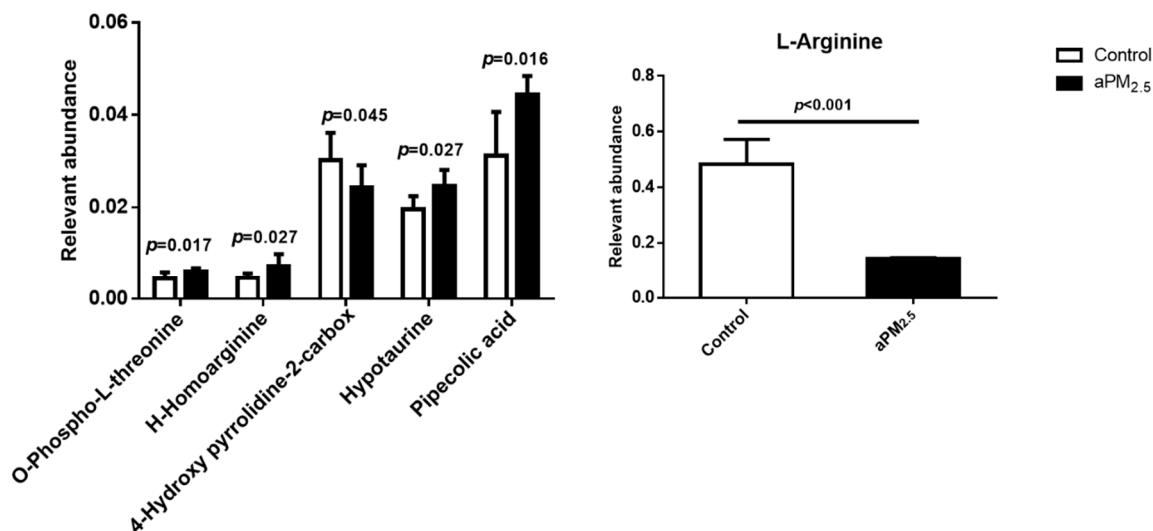


Figure 5. The discriminating metabolites obtained from lung tissue samples in the control and aPM_{2.5} groups by LC-MS/MS analysis. Data were calculated from the ratio of the mean peak areas in the control and aPM_{2.5} groups and normalized to L-norvaline (internal standard); *p* value of independent *t*-test, *n* = 8.

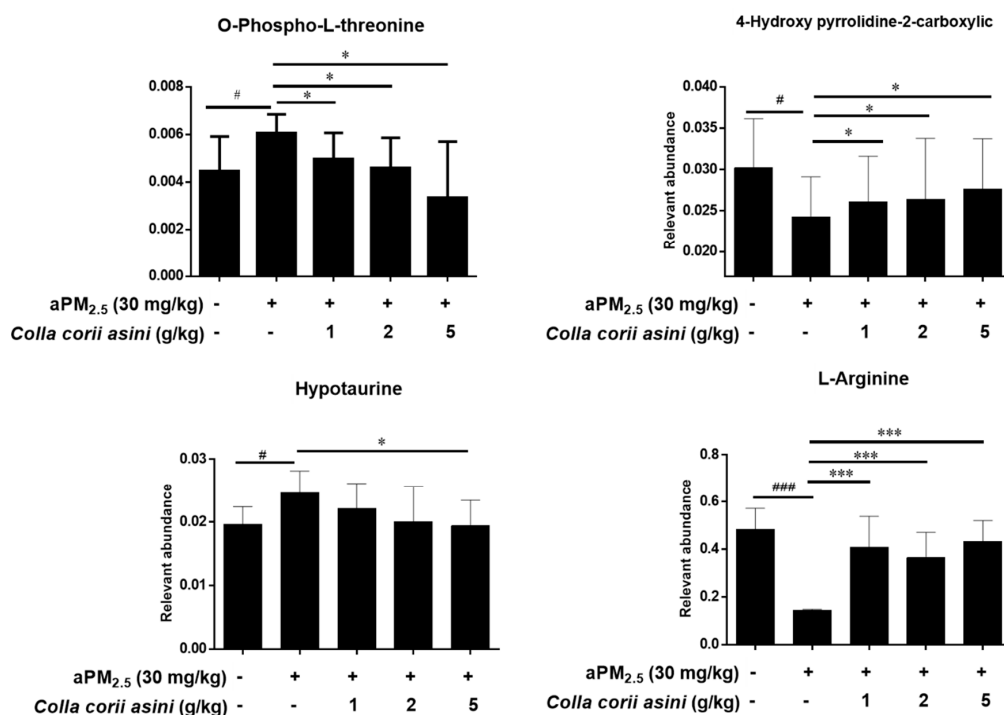


Figure 6. Protective effects of *Colla corii asini* against aPM_{2.5}-induced alteration of amino metabolic profile. Data were calculated from the ratio of the mean peak areas in the aPM_{2.5} and *Colla corii asini* groups and normalized to L-norvaline (internal standard); # *p* < 0.05 and ### *p* < 0.001, versus the control group; * *p* < 0.05 and *** *p* < 0.001, versus the aPM_{2.5} group, *n* = 8.

Expression levels of *Arg-1* and *iNOS* mRNA were determined in the lungs of aPM_{2.5}-exposed rats after 11 weeks to verify their role in the arginine metabolism pathway. The *Arg-1* mRNA level was

increased 1.87-fold ($^{\#} p < 0.05$) compared to the control group, which was reversed to some extent in the *Colla corii asini*-treated groups but the changes were not statistically significant. *Colla corii asini* treatment also reversed the elevated level of *iNOS* induced by aPM_{2.5} (Figure 7).

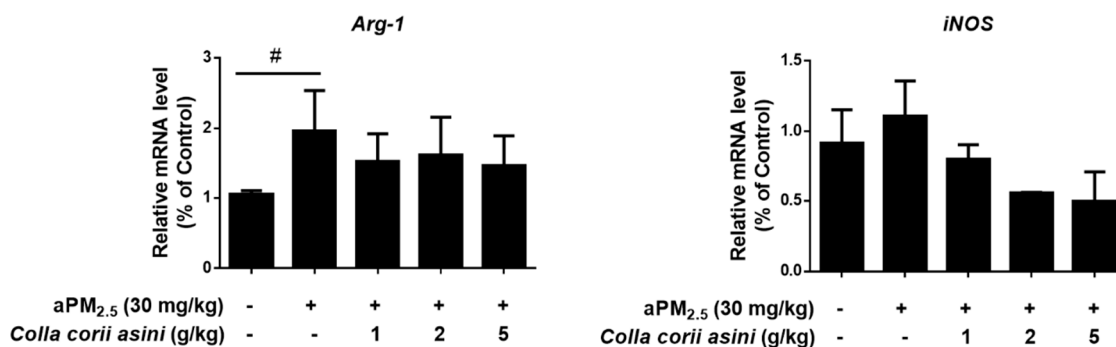


Figure 7. Effects of *Colla corii asini* on the relative gene expression of *Arg-1* and *iNOS* in the lungs of rats subjected to intratracheal instillation of aPM_{2.5} for 11 weeks. Values are reported using the $2^{-\Delta\Delta Ct}$ method and were obtained by comparing with those of the control group and normalized to ACTB (mean \pm SD, $n = 3$). $^{\#} p < 0.05$, versus the control group.

3. Discussion

A large amount of literature evidence supports a robust association between exposure to PM_{2.5} and pulmonary disease morbidity and mortality, therefore PM_{2.5}-induced respiratory system damage has become a serious public health concern [19–21]. Our previous study successfully created a multi-component aPM_{2.5}, based on the size and composition of actual PM_{2.5} collected in Beijing and demonstrated that inhalation of aPM_{2.5} by rats resulted in lung function decline and oxidative stress injuries [22]. In order to further explore the mechanisms of PM_{2.5}-induced lung toxicity, we created an intratracheal instillation-injury animal model using these artificial particles and evaluated intervention with *Colla corii asini*, which has long been used in traditional Asian medicine to treat various ailments, including pulmonary dysfunction [17,23,24].

Our results showed that aPM_{2.5}-induced lung injuries were associated with decreased lung function and linked to inflammation according to a series of biochemical parameters. The results were generally consistent with those from studies reported in the literature [25,26]. We observed that breath flow and volume parameters (tidal volume, expiratory volume, minute ventilation volume, expiratory flow at 50% tidal volume, peak expiratory flow, peak inspiratory flow) increased, while time parameters (relaxation time, expiratory time, inspiratory time) decreased, in animals after exposure to aPM_{2.5}, indicating that the rats were in a state of shortness of breath [27]. The reason for the significant change in the respiratory function of the control group may be due to the irritative damage to the airway caused by the infusion of physiological saline. The results suggested that after intratracheal instillation of aPM_{2.5}, pulmonary ventilation and gas storage function were decreased and airflow was blocked, which might result from pathologic changes such as alveolar height dilatation, alveolar wall rupture and fusion [28].

Published data suggest that ambient PM pollution causes oxidative stress [29] and may influence allergic [30], immunologic [31] and systemic inflammatory responses [32–34]. The results demonstrated that inflammation caused by the administration of aPM_{2.5} led to a substantial increase in the levels of WBC, LYM, MON, NEUT and EOS compared to the controls. To further explore the possible mechanisms of aPM_{2.5}-induced pulmonary inflammation, we investigated the expression of inflammation-related cytokines in vivo at molecular and genetic levels. We observed an increase of pro-inflammatory cytokines (TNF- α , IL-1 β) and a decrease of anti-inflammatory cytokine (IL-10), which were consistent with other published studies [35–37]. In addition, histological examination found inflammatory cell infiltration in the lung tissue.

A metabolomics approach was used to explore novel biomarker metabolites in the lung tissue from rats. This study reports for the first time that O-phospho-L-threonine may play a role in lung damage. Hypotaurine is known to modify the indices of oxidative stress and membrane damage, which is associated with lung adenocarcinoma [38–40]. Pipecolic acid (Pip), a non-protein lysine catabolite, is an important regulator of immunity in animals and plants [41–43]. In our study, the aPM_{2.5} group was characterized by increased levels of O-phospho-L-threonine, H-homoarginine, hypotaurine and pipecolic acid and decreased levels of 4-hydroxy-pyrrolidine-2-carboxylic and L-arginine. Our results demonstrate that arginine metabolism is the most indicative pathway after particle exposure for 11 weeks. Studies have shown that arginase and iNOS may regulate diverse pathways, including production of nitric oxide, polyamines and proline, which are critical components of immune suppression pathways [44–46]. Expression of arginase-1 is commonly believed to promote inflammation, fibrosis and wound healing [47]. *Arg-1* function was inhibited by aPM_{2.5} in our rat model, which might have contributed to the pathogenesis of lung injury [48]. The level of *iNOS* was increased in the aPM_{2.5} group compared to the control but this was not statistically significant. The roles of 4-hydroxy-pyrrolidine-2-carboxylic and H-homoarginine in arginine and proline metabolism still need further research. Studies have shown that L-arginine and its downstream metabolites could modulate innate and adaptive immunity to promote tumor survival and growth [49,50]. Nina E. King et al. have shown that asthmatic responses involve transport and metabolism of arginine by arginase in allergic airway inflammation. Scott J. et al. demonstrated that impairment of the L-arginine metabolism pathway can contribute to exacerbation of airway responsiveness to contractile agents [51]. Taking these observations and our findings together, it can be argued that altered arginine metabolism may represent a broad marker of lung damage and might be an early diagnostic marker of pulmonary disease.

In recent years, numerous traditional Chinese medicines have been found to possess potent pulmonary-protective activities and have attracted considerable interest as potential candidates for the development of novel therapies [17,24,52,53]. Our animal model revealed that *Colla corii asini* (1, 2, 5 g/kg/d, oral, for 11 weeks) inhibited aPM_{2.5}-induced inflammation, reduced infiltration, maintained alveoli structure, inhibited pro-inflammatory cytokines (TNF- α and IL-1 β) and elevated anti-inflammatory cytokine (IL-10) production in the lung. The number of CD8⁺ cytotoxic T cells in the lung correlates with the degree of airflow obstruction, suggesting that these cells cause tissue injury in lung. *Colla corii asini* decreased CD8⁺ level in the presence of aPM_{2.5} and also reversed the imbalance of CD4⁺ / CD8⁺ subsets in rats with airway inflammation. The defense mechanisms might involve the regulation of arginine and nitrogen metabolism pathways, as well as aminoacyl-tRNA biosynthesis. With the exception of H-homoarginine and pipecolic acid, changes in the levels of the other four identified metabolites were reversed by *Colla corii asini*. There were 24 additional discriminating metabolites involved in the protective effect of *Colla corii asini* against aPM_{2.5} injury. According to Michaela Kendall et al. [54], fine airborne urban particles (PM_{2.5}) can sequester serine, asparagine and leucine following immersion in dilute human lavage fluid for short periods and suggested that this may involve lung opsonins, which is consistent with our findings. However, their role in protection against aPM_{2.5}-induced alteration of amino metabolic pathways still needs further research. Our results showed that *Colla corii asini* significantly protected lung function and pathologic changes in response to aPM_{2.5}. Our next study will focus on whether *Colla corii asini* could induce macrophage polarization towards a resolving M2 macrophage phenotype against lung injury.

In summary, our findings suggest that *Colla corii asini* could ameliorate lung function decline, suppress inflammation and regulate the balance of T lymphocyte subsets via suppression of arginase-1 to adjust the perturbed metabolic pathways induced by aPM_{2.5}. Combining metabolomics data with pharmacological assays, we were able to obtain knowledge of the mechanisms of PM_{2.5}-induced lung toxicity and the protective effects of *Colla corii asini* at an holistic level. Additionally, our work confirmed the utility of metabolomics platforms to dissect the underlying efficacy and protective mechanisms of traditional Chinese medicines.

4. Materials and Methods

4.1. Chemical Reagents

aPM_{2.5} samples were provided by Dr. QiMing Wang and obtained from Professor Zhonggao Gao Laboratories (Beijing, China). Samples were produced in accordance with a previous publication [22] using predominantly mesoporous silica nanoparticles (MSN), nitrate (NO₃⁻), sulfate (SO₄²⁺) and chromium (Cr). *Colla corii asini* (Lot: 20150701) was supplied by Shan Dong Donggeiao Co., Ltd. (Shandong, China).

4.2. Animal Handling

Forty male (weighing 180–220 g) specific pathogen-free Sprague–Dawley (SD) rats, aged 6–8 weeks, were obtained from Beijing Vital River Laboratory Animal Technological Company (Beijing, China). All animal studies were conducted at the New Drug Safety Evaluation Center, Institute of Materia Medica, Chinese Academy of Medical Sciences and Peking Union Medical College. Rats were individually housed in suspended steel cages and acclimated in environmentally-controlled rooms (temperature of 20–26 °C; relative humidity of 40–70%; 12 h light/dark cycle) for 2 weeks prior to initiation of dosing, with food and water available *ad libitum*. The experiment protocol were approved by the laboratory animal welfare ethics committee of Beijing Union-Genius Pharmaceutical Technology Development Co., Ltd. (Beijing, China) (No.0000254, Aug. 16, 2016). The facilities achieved the Association for Assessment and Accreditation of Laboratory Animal Care International (AAALAC International) accreditation (1438#) and the animals were maintained according to the 'Guide for the Care and Use of Laboratory Animals (Guide), NRC 2011.'

4.3. Rat model of Intratracheal Instillation of aPM_{2.5} and the Administration of *Colla corii asini*

Dosing formulations of *Colla corii asini* were dissolved in pure deionized water, protected from light and stored at 2–8 °C until administration. aPM_{2.5} was dissolved in physiological saline, ultrasonically broken in a Sonifier cell disruptor and stored at 2–8 °C until administration. SD rats were randomly assigned to the following five groups (8 per group): (I) control group, (II) aPM_{2.5} group, (III–V) aPM_{2.5} + *Colla corii asini* groups (low-, mid- and high-dose groups). Rats in the aPM_{2.5} + *Colla corii asini* groups received *Colla corii asini* daily by oral gavage for 11 weeks at doses of 1, 2 and 5 g/kg body weight, whereas rats in the other two groups were treated with distilled water (10 mL/kg). Twice weekly intratracheal instillation of aPM_{2.5} (30 mg/kg, 1 mL/kg body weight) was used to induce lung injury, using a volume of 1 ml (kg·bw)⁻¹, while the control group received equivalent volumes of physiological saline [55].

4.4. Pulmonary Function Measurement

Respiratory function was measured using a whole body plethysmography system (Emka Technologies, Paris, France) and the raw data were converted using specialized analysis software (IOX 2.9.4.32, Emka Technologies). Briefly, conscious rats were placed in plethysmography chambers for 10–15 min, eliminating data from animals adapting to their environments or sleeping. The test parameters, including respiratory rate (f), expiratory flow at 50% tidal volume (EF50), peak expiratory flow (PEF), peak inspiratory flow (PIF), tidal volume (TV), minute ventilation volume (MV), expiratory volume (EV), inspiratory time (Ti), relaxation time (RT) and expiratory time (Te), were recorded during a 3–8 min period once a week for 11 weeks [56].

4.5. T Lymphocyte Phenotype Analysis of Whole Blood

Fresh whole blood (100 µL in EDTA) was incubated with 5 µL of each antibody for 20 min in the dark, treated with 2 mL ACK Lysis Buffer (Sigma-Aldrich, St. Louis, MO, USA) and then centrifuged at 180 g for 5 min. After two washes with PBS/1% BSA (Sigma-Aldrich), the cells were

resuspended in 2 mL PBS and analyzed immediately via flow cytometry using a FACSCalibur™ system with CellQuest™ software (BD Biosciences, Franklin Lakes, NJ, USA). All T cell samples were stained with APC conjugated mouse anti-rat CD3 antibody (BD Pharmingen, Franklin Lakes, NJ, USA). To determine the CD4⁺/CD8⁺ ratio, cells were stained with FITC conjugated mouse anti-rat CD8 (BD Pharmingen) and PE conjugated mouse anti-rat CD4 (BD Pharmingen) in the same test tube [57,58].

4.6. Bronchoalveolar Lavage Fluid Collection and Analysis

Bronchoalveolar lavage fluid (BALF) was obtained by slow perfusion of cold saline (12 mL) into the left lung three times via tracheal intubation [59]. The BALF was separated by centrifugation at 300 g for 10 min at 4 °C. The cell-free supernatants were assayed for cytokines. Assay kits for TNF- α , IL-1 β and IL-10 were provided by Bio-Plex Pro™ (Hercules, CA, USA). The cytokine levels were measured according to the manufacturer's instructions. The cell pellets were resuspended in WBC dilution buffer (200 μ L) for cell counts and classification. The following parameters were measured using a MEK-7222 K Automated Hematology Analyzer (Nihon-Kodhen Co., Tokyo, Japan): white blood cell (WBC), lymphocyte (LYM), monocyte (MON), neutrophil (NEUT), eosinophil (EOS) and basophil (BAS).

4.7. Lung Histopathology Analysis

Following BALF collection, lung right lobe specimens were removed and fixed with 10% neutral formaldehyde. Tissue blocks were embedded in paraffin and cut into 4- μ m sections using an RM2145 microtome (LEICA, Wetzlar, Germany). The sections were stained with hematoxylin and eosin (H&E) and observed under a light microscope (LEICA).

4.8. LC-MS/MS-Based Metabolomics Analysis

Lung tissues (~50 mg) were prepared by mixing lung tissue homogenate (100 μ L) with acetonitrile containing 0.1 mM norvaline (400 μ L). After centrifugation at 15,000 g for 10 min, a 5 μ L aliquot of the supernatant was injected into a LC-MS/MS system. The separation of lung components was performed on an ACQUITY UPLC BEH C18 column (3.5 m, 2.1 \times 100 mm, Waters Corp, Milford, MA, USA). The mobile phase consisted of two solvents: mobile phase A [99.9% water and 0.1% aqueous formic acid (*v/v*) containing 10 mM ammonium acetate] and mobile phase B (49.95% acetonitrile, 49.95% isopropanol and 0.1% aqueous formic acid (*v/v*) containing 10 mM ammonium acetate). The running method was as described in a previous study [60]. The metabolites were quantified using an ACQUITY UPLC (Eksigent LC100) system coupled with a hybrid quadrupole time-of-flight mass spectrometer (Triple TOF 5600+, AB SCIEX). Metabolomics databases (Madison Metabolomics Consortium Database and METLIN) were searched to identify the structures of high-contribution score metabolites. MassLynx software (Waters Corp.) was used to acquire the chromatogram and mass spectrometric data in centroid format. The dataset was exported into SIMCA-P+ 12.0 (Umetrics, Kinnelon, NJ, USA) for further analysis after generation of a multivariate data matrix, as previously described [61].

4.9. Quantitative Reverse-Transcriptase DNA Polymerase Chain Reaction (qRT-PCR) Analysis

A TRIzol® Plus RNA Purification Kit (Invitrogen, Hillsboro, OR, USA), following the manufacturer's instructions, was used to extract total RNA from the right lung tissues of SD rats. Total RNA (0.5 μ g) was reverse transcribed into cDNA using a HiScript II Q RT SuperMix IIa kit (Vazyme, Nanjing, China). PCR was carried out on a LightCycler® 480 II Real-time PCR Instrument (Roche, Switzerland) with QuantiFast® SYBR® Green PCR Master Mix (Qiagen, Germany). The primer sequences were designed in the laboratory and synthesized by Generay Biotech (Generay, Shanghai, China) based on the mRNA sequences obtained from the NCBI database as described in Table 2. The mRNA expression levels were normalized to β -actin (ACTB) and were calculated using the $2^{-\Delta\Delta C_t}$ method [52].

Table 2. Sequences of primers used for qRT-PCR.

Gene Name	Forward Primer	Reverse Primer
<i>TNF-α</i>	ACCAGCAGATGGGCTGTA	CTCCTGGTATGAAATGGCAA
<i>IL-1β</i>	CAAGGAGAGACAAGCAACG	TTCATCACACAGGACAGGTAT
<i>IL-10</i>	ACTGGACTGCAGGACATA	TTTGGAGAGAGGTACAAACGA
<i>iNOS</i>	TTGCTTCTGTGCTAATGCG	TCCGACTTTCTGTCTCAGTA
<i>Arg-1</i>	TCGTACTGTGAACACGGC	GGTAGTCAGTCTCTGGCTTAT
<i>ACTB</i>	CCACCATGTACCCAGGCATT	CGGACTCATCGTACTCTCTGC

4.10. Statistical Analysis

The experimental data are presented as mean \pm standard deviation (SD). SPSS 22.0 and GraphPad Prism 6.0 were used for statistical analysis and graph generation. Shapiro-Wilk test was first used to verify the normality of data. Comparisons between two groups were performed using a two-tailed unpaired Student's t test. One-way analysis of variance (ANOVA) followed by Tukey's post hoc tests were used to compare more than two populations. Significant differences were attributed to values with * $p < 0.05$, ** $p < 0.01$ and *** $p < 0.001$.

Supplementary Materials: Supplementary materials can be found at <http://www.mdpi.com/1422-0067/20/1/55/s1>.

Author Contributions: H.J. and J.G. conceived and designed research; P.Z. and Y.L. performed experiments; T.L., P.Z., Y.L. and G.H. analyzed data; T.L., P.Z., Y.L., J.W. and A.W., interpreted experimental results; T.L., P.Z. and Y.L. prepared figures; T.L. drafted manuscript; T.L., H.Y. and H.J. edited and revised manuscript; H.J. approved the final version of manuscript.

Funding: Financial support for this research was received from the National Science and Technology Major Projects for "Major New Drugs Innovation Development", Chinese Academy of Medical Sciences-CAMS Innovation (CAMS-I2M) and Youth Research Fund of Peking Union Medical College in 2017 (grant numbers: 2018ZX09201017-005, 2017-I2M-1-011, 2017350004).

Acknowledgments: We would like to thank the team of Professor Zhong-Ze Fang at Tianjin Medical University for helping with the metabolic measurements.

Conflicts of Interest: The authors have declared that there are no conflicts of interest.

Abbreviations

aPM	Artificial particular matter
ACTB	β -actin
BALF	Bronchoalveolar lavage fluid
LC-MS/MS	Liquid chromatograph-mass spectrometer/ mass spectrometer
IL	Interleukin

References

- Di, Q.; Wang, Y.; Zanobetti, A.; Wang, Y.; Koutrakis, P.; Choirat, C.; Dominici, F.; Schwartz, J.D. Air Pollution and Mortality in the Medicare Population. *N. Engl. J. Med.* **2017**, *376*, 2513–2522. [[CrossRef](#)] [[PubMed](#)]
- Landrigan, P.J.; Fuller, R.; Acosta, N.J.R.; Adeyi, O.; Arnold, R.; Basu, N.; Baldé, A.B.; Bertollini, R.; Bose-O'Reilly, S.; Boufford, J.I.; et al. The Lancet Commission on pollution and health. *Lancet* **2018**, *391*, 462–512. [[CrossRef](#)]
- Landrigan, P.J. Air pollution and health. *Lancet Public Health* **2017**, *2*, e4–e5. [[CrossRef](#)]
- Guan, W.-J.; Zheng, X.-Y.; Chung, K.F.; Zhong, N.-S. Impact of air pollution on the burden of chronic respiratory diseases in China: Time for urgent action. *Lancet* **2016**, *388*, 1939–1951. [[CrossRef](#)]
- Yin, P.; He, G.; Fan, M.; Chiu, K.Y.; Fan, M.; Liu, C.; Xue, A.; Liu, T.; Pan, Y.; Mu, Q. Particulate air pollution and mortality in 38 of China's largest cities: Time series analysis. *BMJ* **2017**, *356*, j667. [[CrossRef](#)] [[PubMed](#)]
- Wang, C.; Xu, J.; Yang, L.; Xu, Y.; Zhang, X.; Bai, C.; Kang, J.; Ran, P.; Shen, H.; Wen, F. Prevalence and risk factors of chronic obstructive pulmonary disease in China (the China Pulmonary Health [CPH] study): A national cross-sectional study. *Lancet* **2018**, *391*, 1706–1717. [[CrossRef](#)]

7. Ni, L.; Chuang, C.-C.; Zuo, L. Fine particulate matter in acute exacerbation of COPD. *Front. Physiol.* **2015**, *6*, 294. [[CrossRef](#)] [[PubMed](#)]
8. Cosselman, K.E.; Navas-Acien, A.; Kaufman, J.D. Environmental factors in cardiovascular disease. *Nat. Rev. Cardiol.* **2015**, *12*, 627. [[CrossRef](#)]
9. Nel, A. Air pollution-related illness: Effects of particles. *Science* **2005**, *308*, 804–806. [[CrossRef](#)]
10. Wang, H.; Naghavi, M.; Allen, C.; Barber, R.M.; Bhutta, Z.A.; Carter, A.; Casey, D.C.; Charlson, F.J.; Chen, A.Z.; Coates, M.M. Global, regional, and national life expectancy, all-cause mortality, and cause-specific mortality for 249 causes of death, 1980–2015: A systematic analysis for the Global Burden of Disease Study 2015. *Lancet* **2016**, *388*, 1459–1544. [[CrossRef](#)]
11. Liu, M.; Tan, H.; Zhang, X.; Liu, Z.; Cheng, Y.; Wang, D.; Wang, F. Hematopoietic effects and mechanisms of Fufang ejiao jiang on radiotherapy and chemotherapy-induced myelosuppressed mice. *J. Ethnopharmacol.* **2014**, *152*, 575–584. [[CrossRef](#)] [[PubMed](#)]
12. Chen, H.; You, J.; Tian, S.; Zhang, Y.; Feng, M. Overview of pharmacological and clinical study on compound Ejiao Jiang. *China J. Chin. Mater. Med.* **2012**, *37*, 3021–3023.
13. Wu, H.; Yang, F.; Cui, S.; Qin, Y.; Liu, J.; Zhang, Y. Hematopoietic effect of fractions from the enzyme-digested *colla corii asini* on mice with 5-fluorouracil induced anemia. *Am. J. Chin. Med.* **2007**, *35*, 853–866. [[CrossRef](#)] [[PubMed](#)]
14. Wang, D.; Liu, M.; Cao, J.; Cheng, Y.; Zhuo, C.; Xu, H.; Tian, S.; Zhang, Y.; Zhang, J.; Wang, F. Effect of *Colla corii asini* (E'jiao) on D-galactose induced aging mice. *Biol. Pharm. Bull.* **2012**, *35*, 2128–2132. [[CrossRef](#)] [[PubMed](#)]
15. Zhang, X.; Wang, F.; Li, B.; Yang, Y.; Tian, S.; Li, Z. Effect of colla corri asini on immune function in mice. *Sci. Technol. Food Ind.* **2011**, *32*, 400–402.
16. Zhang, Z.; Ma, Y.; Hu, J.; Lan, H.; Zhang, Y.; Yao, C. Reverse effect of Ejiao (colla corri asini) on imbalance of Th17/Treg subsets of mice with airway inflammation. *Shandong Med. J.* **2018**, *6*, 11–14.
17. Piaopiao, Z.; Yahao, L.; Xiaodan, Y.; Jinfeng, W.; Hongtao, J.; Aiping, W. Protective effects of *Colla corii asini* in on artificial fine particulate matter-induced respiratory system injury in rats. *Carcinog. Teratog. Mutagen.* **2017**, *29*, 346–351.
18. Zhang, W.; Sun, Y.; Zhuang, G.; Xu, D. Characteristics and seasonal variations of PM_{2.5}, PM₁₀, and TSP aerosol in Beijing. *Biomed. Environ. Sci.* **2006**, *19*, 461.
19. Jerrett, M. Atmospheric science: The death toll from air-pollution sources. *Nature* **2015**, *525*, 330. [[CrossRef](#)]
20. Cohen, A.J.; Brauer, M.; Burnett, R.; Anderson, H.R.; Frostad, J.; Estep, K.; Balakrishnan, K.; Brunekreef, B.; Dandona, L.; Dandona, R. Estimates and 25-year trends of the global burden of disease attributable to ambient air pollution: An analysis of data from the Global Burden of Diseases Study 2015. *Lancet* **2017**, *389*, 1907–1918. [[CrossRef](#)]
21. Raaschou-Nielsen, O.; Andersen, Z.J.; Beelen, R.; Samoli, E.; Stafoggia, M.; Weinmayr, G.; Hoffmann, B.; Fischer, P.; Nieuwenhuijsen, M.J.; Brunekreef, B. Air pollution and lung cancer incidence in 17 European cohorts: Prospective analyses from the European Study of Cohorts for Air Pollution Effects (ESCAPE). *Lancet Oncol.* **2013**, *14*, 813–822. [[CrossRef](#)]
22. Yan, X.D.; Wang, Q.M.; Cai, T.; Jin, H.T.; Han, Y.X.; Zhang, J.L.; Yu, X.M.; Hou, Q.; Zhang, P.P.; Wang, A.P. Polydatin protects the respiratory system from PM_{2.5} exposure. *Sci. Rep.* **2017**, *7*, 1–11. [[CrossRef](#)] [[PubMed](#)]
23. Zhao, F.; Dong, J.; Cui, Y.; Xie, J.; Wu, S. The effect of Ejiao on airway inflammation and Th1/Th2 cytokines in serum of asthmatic rats. *Chin. J. Exp. Tradit. Med. Form.* **2006**, *12*, 59–61.
24. Zhang, Z.; Li, N.; Liu, Q.; Ma, Y.; Zhang, Y.; Lan, H.-Y.; Yao, C.-F. Protective Effect of Ejiao on COPD Model Mice and the Effect on MMP-2, MMP-9 and TGF- β 1 Levels. *Genom. Appl. Biol.* **2018**, *37*, 1813–1819.
25. De Fcajfc, A.J.; Der Plaat, D.A.; de Jong, K.; van Diemen, C.; Dirkje, S.; Nedeljkovic, I.; van Duijn, C.; Amin, N.; La Bastide-van Gemert, S.; Maaik Vries, M. Long-term air pollution exposure, genome-wide DNA methylation and lung function in the LifeLines cohort study. *Environ. Health Perspect.* **2018**, *126*, 027004.
26. Bergstra, A.D.; Brunekreef, B.; Burdorf, A. The effect of industry-related air pollution on lung function and respiratory symptoms in school children. *Environ. Health* **2018**, *17*, 30. [[CrossRef](#)] [[PubMed](#)]
27. Mu, L.; Deng, F.; Tian, L.; Li, Y.; Swanson, M.; Ying, J.; Browne, R.W.; Rittenhouse-Olson, K.; Zhang, J.J.; Zhang, Z.-F. Peak expiratory flow, breath rate and blood pressure in adults with changes in particulate matter air pollution during the Beijing Olympics: A panel study. *Environ. Res.* **2014**, *133*, 4–11. [[CrossRef](#)]

28. Sigaud, S.; Goldsmith, C.-A.W.; Zhou, H.; Yang, Z.; Fedulov, A.; Imrich, A.; Kobzik, L. Air pollution particles diminish bacterial clearance in the primed lungs of mice. *Toxicol. Appl. Pharmacol.* **2007**, *223*, 1–9. [[CrossRef](#)] [[PubMed](#)]
29. Li, N.; Sioutas, C.; Cho, A.; Schmitz, D.; Misra, C.; Sempf, J.; Wang, M.; Oberley, T.; Froines, J.; Nel, A. Ultrafine particulate pollutants induce oxidative stress and mitochondrial damage. *Environ. Health Perspect.* **2003**, *111*, 455. [[CrossRef](#)]
30. Diaz-Sanchez, D.; Proietti, L.; Polosa, R. Diesel fumes and the rising prevalence of atopy: An urban legend? *Curr. Allergy Asthma Rep.* **2003**, *3*, 146–152. [[CrossRef](#)] [[PubMed](#)]
31. Burchiel, S.W.; Lauer, F.T.; McDonald, J.D.; Reed, M.D. Systemic immunotoxicity in AJ mice following 6-month whole body inhalation exposure to diesel exhaust. *Toxicol. Appl. Pharmacol.* **2004**, *196*, 337–345. [[CrossRef](#)] [[PubMed](#)]
32. van Eeden, S.F.; Hogg, J.C. Systemic inflammatory response induced by particulate matter air pollution: The importance of bone-marrow stimulation. *J. Toxicol. Environ. Health Part A* **2002**, *65*, 1597–1613. [[CrossRef](#)] [[PubMed](#)]
33. Jing, Y.; Zhang, H.; Cai, Z.; Zhao, Y.; Wu, Y.; Zheng, X.; Liu, Y.; Qin, Y.; Gu, M.; Jin, J. Bufei huoxue capsule attenuates PM_{2.5}-induced pulmonary inflammation in mice. *Evid.-Based Complement. Altern. Med.* **2017**, *2017*, 1575793. [[CrossRef](#)] [[PubMed](#)]
34. Wong, T.-H.; Lee, C.-L.; Su, H.-H.; Lee, C.-L.; Wu, C.-C.; Wang, C.-C.; Sheu, C.-C.; Lai, R.-S.; Leung, S.-Y.; Lin, C.-C. A prominent air pollutant, Indeno [1, 2, 3-cd] pyrene, enhances allergic lung inflammation via aryl hydrocarbon receptor. *Sci. Rep.* **2018**, *8*, 5198. [[CrossRef](#)] [[PubMed](#)]
35. Zhang, R.; Dai, Y.; Zhang, X.; Niu, Y.; Meng, T.; Li, Y.; Duan, H.; Bin, P.; Ye, M.; Jia, X. Reduced pulmonary function and increased pro-inflammatory cytokines in nanoscale carbon black-exposed workers. *Part. Fibre Toxicol.* **2014**, *11*, 73. [[CrossRef](#)] [[PubMed](#)]
36. Xu, F.; Qiu, X.; Hu, X.; Shang, Y.; Pardo, M.; Fang, Y.; Wang, J.; Rudich, Y.; Zhu, T. Effects on IL-1 β signaling activation induced by water and organic extracts of fine particulate matter (PM 2.5) in vitro. *Environ. Pollut.* **2018**, *237*, 592–600. [[CrossRef](#)] [[PubMed](#)]
37. Sharma, A.K.; Fernandez, L.G.; Awad, A.S.; Kron, I.L.; Laubach, V.E. Proinflammatory response of alveolar epithelial cells is enhanced by alveolar macrophage-produced TNF- α during pulmonary ischemia-reperfusion injury. *Am. J. Physiol.-Lung Cell. Mol. Physiol.* **2007**, *293*, L105–L113. [[CrossRef](#)] [[PubMed](#)]
38. Gossai, D.; Lau-Cam, C.A. The effects of taurine, taurine homologs and hypotaurine on cell and membrane antioxidative system alterations caused by type 2 diabetes in rat erythrocytes. *Adv. Exp. Med. Biol.* **2009**, *643*, 359–368.
39. Bucak, M.N.; Tuncer, P.B.; Sariözkan, S.; Ulutaş, P.A.; Çoyan, K.; Başpınar, N.; Özkalp, B. Effects of hypotaurine, cysteamine and aminoacids solution on post-thaw microscopic and oxidative stress parameters of Angora goat semen. *Res. Vet. Sci.* **2009**, *87*, 468–472. [[CrossRef](#)]
40. Pradhan, M.P.; Desai, A.; Palakal, M.J. Systems biology approach to stage-wise characterization of epigenetic genes in lung adenocarcinoma. *BMC Syst. Biol.* **2013**, *7*, 141. [[CrossRef](#)]
41. Navarova, H.; Bernsdorff, F.; Doring, A.C.; Zeier, J. Pipecolic Acid, an Endogenous Mediator of Defense Amplification and Priming, Is a Critical Regulator of Inducible Plant Immunity. *Plant Cell* **2012**, *24*, 5123–5141. [[CrossRef](#)] [[PubMed](#)]
42. Wang, C.; Liu, R.; Lim, G.-H.; de Lorenzo, L.; Yu, K.; Zhang, K.; Hunt, A.G.; Kachroo, A.; Kachroo, P. Pipecolic acid confers systemic immunity by regulating free radicals. *Sci. Adv.* **2018**, *4*, eaar4509. [[CrossRef](#)]
43. Chang, Y.-F. Pipecolic acid pathway: The major lysine metabolic route in the rat brain. *Biochem. Biophys. Res. Commun.* **1976**, *69*, 174–180. [[CrossRef](#)]
44. Bogdan, C. Nitric oxide and the immune response. *Nat. Immunol.* **2001**, *2*, 907. [[CrossRef](#)] [[PubMed](#)]
45. Förstermann, U.; Sessa, W.C. Nitric oxide synthases: Regulation and function. *Eur. Heart J.* **2011**, *33*, 829–837. [[CrossRef](#)] [[PubMed](#)]
46. Bronte, V.; Zanovello, P. Regulation of immune responses by L-arginine metabolism. *Nat. Rev. Immunol.* **2005**, *5*, 641. [[CrossRef](#)] [[PubMed](#)]
47. Pesce, J.T.; Ramalingam, T.R.; Mentink-Kane, M.M.; Wilson, M.S.; El Kasmi, K.C.; Smith, A.M.; Thompson, R.W.; Cheever, A.W.; Murray, P.J.; Wynn, T.A. Arginase-1-expressing macrophages suppress Th2 cytokine-driven inflammation and fibrosis. *PLoS Pathog.* **2009**, *5*, e1000371. [[CrossRef](#)]

48. Listed, N. Arginine metabolism: Enzymology, nutrition, and clinical significance. Proceedings of a symposium dedicated to the memory of Vernon R. Young. April 5–6, 2004. Bermuda. *J. Nutr.* **2004**, *134*, 2741S–2897S.
49. Geiger, R.; Rieckmann, J.C.; Wolf, T.; Basso, C.; Feng, Y.; Fuhrer, T.; Kogadeeva, M.; Picotti, P.; Meissner, F.; Mann, M. L-arginine modulates T cell metabolism and enhances survival and anti-tumor activity. *Cell* **2016**, *167*, 829–842. [[CrossRef](#)]
50. Feun, L.; You, M.; Wu, C.; Kuo, M.; Wangpaichitr, M.; Spector, S.; Savaraj, N. Arginine deprivation as a targeted therapy for cancer. *Curr. Pharm. Des.* **2008**, *14*, 1049–1057. [[CrossRef](#)]
51. Scott, J.; Chen, R.; North, M.; Urch, B.; Silverman, F.; Grasemann, H.; Chow, C.-W. Alterations of Arginine Metabolism and Lung Function Following Acute Exposure of Mice to Concentrated Ambient Fine Particulate Matter and Ozone. In *D106. Cellular and Molecular Mechanisms of Environmental and Occupational Exposures*; American Thoracic Society: New York, NY, USA, 2018; p. A7560.
52. Kim, K.H.; Kim, E.J.; Kwun, M.J.; Lee, J.Y.; Bach, T.T.; Eum, S.M.; Choi, J.Y.; Cho, S.; Kim, S.-J.; Jeong, S.-I. Suppression of lung inflammation by the methanol extract of *Spilanthes acmella* Murray is related to differential regulation of NF- κ B and Nrf2. *J. Ethnopharmacol.* **2018**, *217*, 89–97. [[CrossRef](#)] [[PubMed](#)]
53. Liang, D.; Sun, Y.; Shen, Y.; Li, F.; Song, X.; Zhou, E.; Zhao, F.; Liu, Z.; Fu, Y.; Guo, M. Shikonin exerts anti-inflammatory effects in a murine model of lipopolysaccharide-induced acute lung injury by inhibiting the nuclear factor-kappaB signaling pathway. *Int. Immunopharmacol.* **2013**, *16*, 475–480. [[CrossRef](#)] [[PubMed](#)]
54. Kendall, M. Fine airborne urban particles (PM_{2.5}) sequester lung surfactant and amino acids from human lung lavage. *Am. J. Physiol. Lung Cell Mol. Physiol.* **2007**, *293*, L1053–L1058. [[CrossRef](#)] [[PubMed](#)]
55. Stoeger, T.; Reinhard, C.; Takenaka, S.; Schroepfel, A.; Karg, E.; Ritter, B.; Heyder, J.; Schulz, H. Instillation of six different ultrafine carbon particles indicates a surface area threshold dose for acute lung inflammation in mice. *Environ. Health Perspect.* **2005**, *114*, 328–333. [[CrossRef](#)] [[PubMed](#)]
56. Happel, C.; Lachmann, N.; Škuljec, J.; Wetzke, M.; Ackermann, M.; Brenig, S.; Mucci, A.; Jirmo, A.C.; Groos, S.; Mirenska, A. Pulmonary transplantation of macrophage progenitors as effective and long-lasting therapy for hereditary pulmonary alveolar proteinosis. *Sci. Transl. Med.* **2014**, *6*, 250ra113. [[CrossRef](#)] [[PubMed](#)]
57. Hertz-Picciotto, I.; Herr, C.E.; Yap, P.-S.; Dostál, M.; Shumway, R.H.; Ashwood, P.; Lipsett, M.; Joad, J.P.; Pinkerton, K.E.; Šrám, R.J. Air pollution and lymphocyte phenotype proportions in cord blood. *Environ. Health Perspect.* **2005**, *113*, 1391. [[CrossRef](#)] [[PubMed](#)]
58. Guo, L.; Zhang, Z. Immunotoxicity of traffic related fine particles to human peripheral blood lymphocytes and calcium signal mechanism. *J. Environ. Health* **2010**, *27*, 946–949.
59. Ma-Hock, L.; Farias, P.M.; Hofmann, T.; Andrade, A.C.; Silva, J.N.; Arnaud, T.M.; Wohlleben, W.; Strauss, V.; Treumann, S.; Chaves, C. Short term inhalation toxicity of a liquid aerosol of glutaraldehyde-coated CdS/Cd(OH)₂ core shell quantum dots in rats. *Toxicol. Lett.* **2014**, *225*, 20–26. [[CrossRef](#)]
60. Fang, Z.-Z.; Krausz, K.W.; Tanaka, N.; Li, F.; Qu, A.; Idle, J.R.; Gonzalez, F.J. Metabolomics reveals trichloroacetate as a major contributor to trichloroethylene-induced metabolic alterations in mouse urine and serum. *Arch. Toxicol.* **2013**, *87*, 1975–1987. [[CrossRef](#)]
61. Fang, Z.-Z.; Tanaka, N.; Lu, D.; Jiang, C.-T.; Zhang, W.-H.; Zhang, C.; Du, Z.; Fu, Z.-W.; Gao, P.; Cao, Y.-F. Role of the lipid-regulated NF- κ B/IL-6/STAT3 axis in alpha-naphthyl isothiocyanate-induced liver injury. *Arch. Toxicol.* **2017**, *91*, 2235–2244. [[CrossRef](#)]

